A particle/collision model of seismic data

Kris Innanen

ABSTRACT

It can occasionally be a valuable exercise to take a familiar phenomenon and observe it from a different point of view. It turns out, for instance, that in the right frame of reference, waves in a VSP experiment seem to act like particles, drifting freely or accelerating in a potential, and thereafter colliding, sticking together, and spontaneously disintegrating. In fact, all of the important properties of simple wave phenomena (phase velocities, propagation directions, amplitudes, reflection and transmission coefficients) are correctly captured by speaking of the experiment entirely in terms of a system of colliding particles (with well-defined, though notional, masses, velocities, and momenta). In the same framework, a seismic *event*, meaning a coherent arrival of wave energy to which we assign a well-defined history of propagation, reflection, and transmission, can be represented in one of two ways. Either a single particle, whose "world-line" is free to move both forwards and backwards in time, or several particles interacting through a specified set of the aforementioned productions and annihilations.

INTRODUCTION

Let us take one of the simplest possible seismic experiments, the zero-offset VSP survey, and imagine that we experience it occurring in an unusual way. Rather than seeing it as a set of seismic amplitudes, available to us over a defined depth interval, evolving as we step forward through time, let us take the reverse view. Let us imagine we perceive the same experiment as a set of amplitudes over a defined time interval, evolving as we step forward through depth. Pretend, in other words, that we experience depth the way we normally experience time, and vice versa.

When we do this, something interesting happens. We find that we may treat seismic disturbances as if they were colliding mechanical particles, with well-defined—though notional—masses and velocities. The collisions occur at points of reflection and transmission, and all wave quantities, prior and posterior to these reflections and transmissions, are correctly predicted by assuming that each collision is mass- and momentum-conserving.

Once we have placed ourselves in a position to interpret seismic phenomena in terms of particles, a lot of ideas from the electrodynamic interaction of electrons and photons become available to us for possible translation to the seismic problem. One of the most interesting examples along these lines is that an individual *event* (i.e., a portion of the measured seismic wave field to which we assign an arrival time, an amplitude, and a well-defined history of propagation and interaction in the Earth) can be viewed as being the consequence of either (1) a sequence of creations, collisions, and annihilations of *several* particles, all moving forward in time, or (2) a *single* particle with a propagation history that moves both forward and backward in time.

REFLECTION AND TRANSMISSION: MASS- AND MOMENTUM-CONSERVING COLLISIONS

Consider the 1D model of a zero-offset VSP experiment in Figure 1, in which the subsurface contains a single reflector at depth z_1, above which waves propagate with velocity c_0, and below which waves propagate with velocity c_1. Receivers are located at depths z_g within the well (we will assume that a suite of receivers are available, reasonably densely spaced, both above and below the interface). A downgoing unit impulse passes $z = 0$ at $t = 0$. The response at z_g is as follows. If $z_g < z_1$, it involves two arrivals, a direct downgoing wave of amplitude 1 and an upgoing wave of amplitude R, whereas if $z_g > z_1$, it involves one arrival, a downgoing wave of amplitude T (see Figure 1).
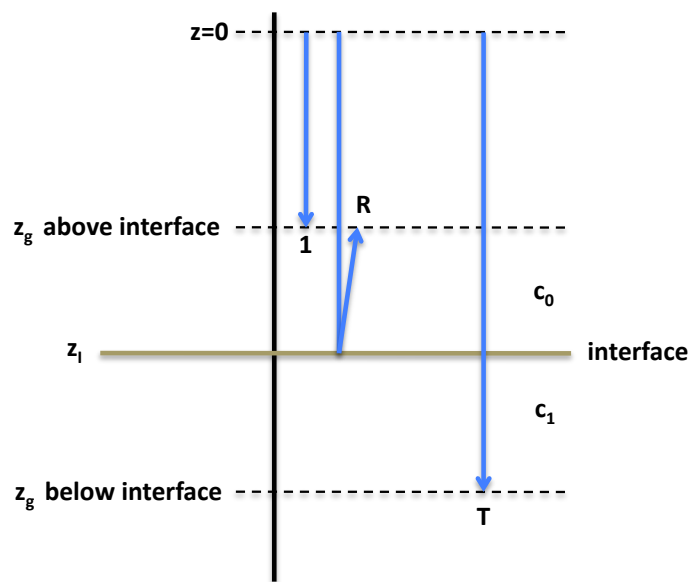

FIG. 1. 1D, normal incidence VSP survey configuration in a medium with a single interface.

Suppose we were to make a movie out of the results of this experiment, assembled as follows. Each frame of the movie is a seismic trace, i.e., the wave field over the full time interval, at a given z_g. We create a suite of movie frames by letting z_g vary from $z_g = 0$ up to some value significantly greater than z_1. We arrange the frames in order from smallest z_g to largest, and run it. Figure 2 contains five of these frames arranged sequentially to provide the general look of the movie—which is that the recorded arrivals appear to drift around along the fixed time axis, occasionally vanishing. The model we are espousing involves imagining that these drifting wave entities represent particles which interact mechanically.

Because the direct wave (which is of unit amplitude) takes longer to arrive the deeper along z_g the receiver is, the disturbance on the left appears to drift to the right with a uniform apparent velocity—meaning the rate of motion along the time axis per unit change in depth. Meanwhile, the reflection from z_1 arrives at maximally late times when z_g is small, and as depth increases its travel path shortens, and hence the right-most arrival appears to drift to

the left. When $z_g = z_1$ the two approaching arrivals coincide. For z_g values larger than z_1, only one arrival, the transmitted wave, remains, and since it propagates downward, it retains the right-moving motion of the direct wave, though, since $c_1 \neq c_0$, it does so at a different apparent velocity.
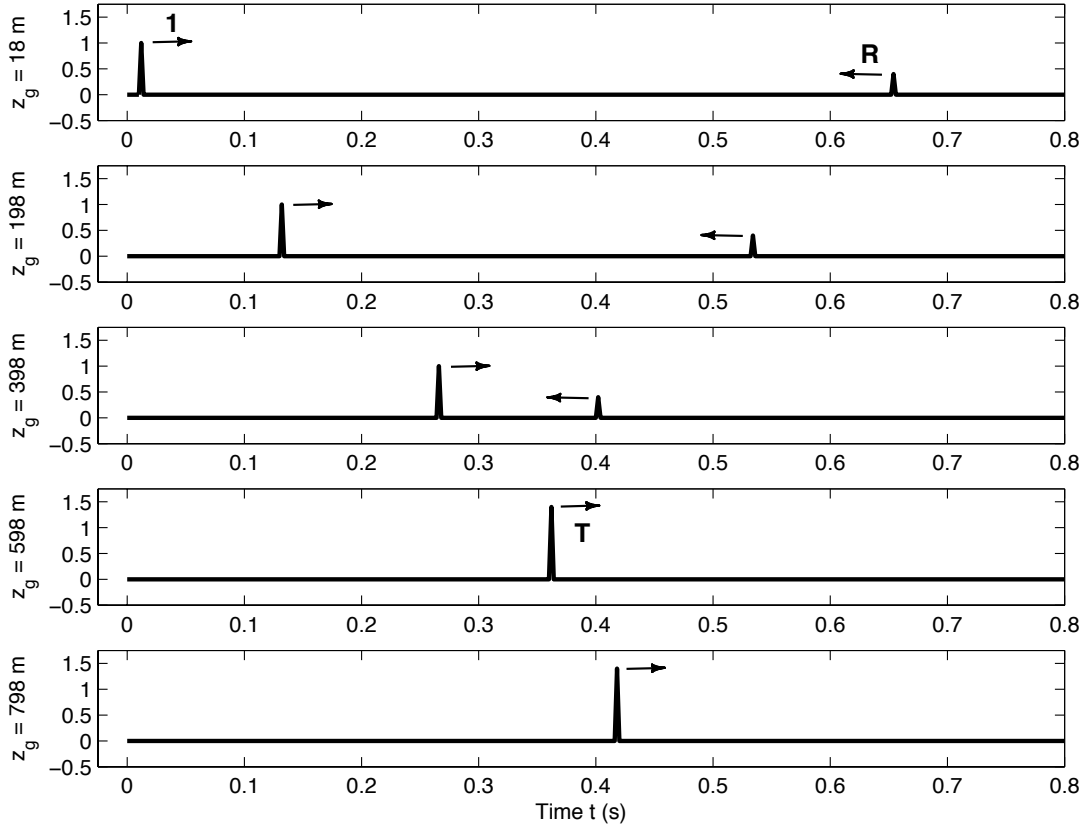

FIG. 2. Collision view of VSP data; 5 snapshots at increasing depth. Bottom two panels are depths below interface $z_1 = 500$m.

To the eye, the movie in Figure 2 appears to depict two objects, one large and one small, moving towards each other at equal and opposite rates. They appear to collide at the apparent time $z_g = z_1$, whereafter, stuck together, they proceed together in the same direction that the original larger object had, but more slowly. If we were to put two carts of different masses on a track and set them on a collision course, and if we could arrange to have them lock together upon colliding, we might expect to see something like Figure 2 happen.

The masses and velocities of two *carts* prior and posterior to a collision obey clear rules, to wit, their masses and momenta before and after the collision are conserved. Let us establish the extent to which the "particles" in the VSP movie can be seen as following rules of this kind, i.e., *quantitatively* behaving like the two carts.

This will require mathematical representation of the seismic data. The data taken by a

receiver at $z_g < z_1$ may be modeled as

$$D(z_g < z_I, t) = 1 \times \delta \left(t - \frac{z_g}{c_0} \right) + R \times \delta \left(t - \frac{2z_1 - z_g}{c_0} \right), \tag{1}$$

and the data taken by a receiver at $z_g > z_1$ as

$$D(z_g > z_I, t) = T \times \delta \left(t - \frac{z_1}{c_0} - \frac{z_g - z_1}{c_1} \right), \tag{2}$$

where $R = (c_1 - c_0)/(c_1 + c_0)$ and $T = 2c_1/(c_0 + c_1)$. With these in hand, we may determine the rates at which the objects in the VSP movie in Figure 2 drift—that is, how quickly along the time axis the wave moves as z_g grows. We will find, not surprisingly, that these rates are proportional to the reciprocals of the actual wave velocities c_0 and c_1, that is they correspond with the vertical slownesses of the media. Consider first the argument of the delta function representing the direct wave, the first term on the right-hand side of equation (1). We are, evidently, right on top of the event if, for a given z_g, the time is

$$t = \frac{z_g}{c_0}. \tag{3}$$

If z_g changes by a positive amount Δz_g, to track the peak of the event we must alter t by Δt such that the argument in first term on the right hand side of equation (1) remains nil, i.e.,

$$t + \Delta t = \frac{z_g + \Delta z_g}{c_0}, \tag{4}$$

hence

$$\Delta t = \frac{\Delta z_g}{c_0}. \tag{5}$$

The apparent velocity with which the direct wave appears to drift in our movie must be $v_{\mathrm{D}} = \Delta t / \Delta z_g$, hence from equation (5) we obtain

$$v_{\mathrm{D}} = \frac{\Delta t}{\Delta z_g} = \frac{1}{c_0}. \tag{6}$$

The same analysis on the reflected event, as a result of the negative sign in front of the z_g in the argument of the second term on the right-hand side of equation (1) produces the same speed and opposite direction:

$$v_{\mathrm{R}} = -\frac{1}{c_0}, \tag{7}$$

and for the transmitted wave we have

$$v_{\mathrm{T}} = \frac{1}{c_1}. \tag{8}$$

With the apparent velocities in hand, and an interest in characterizing the system in terms of mechanical quantities such as momentum, we must next decide what the mass of one of these "particles" is. A neat and simple definition is that the mass of the notional particle is the amplitude of the disturbance. Let us consider this to be a postulate of the model, assuming that gradually its appropriateness will become clear. We let

$$
\begin{aligned}
m_D &\equiv 1, \\
m_R &\equiv R, \\
m_T &\equiv T,
\end{aligned}
\tag{9}
$$

represent the masses of the three particles*. Then, a statement of the conservation of mass of the colliding system would simply be that the sum of the masses of the two particles prior to the collision must equal the mass of the single particle after the collision:

$$
m_D + m_R = m_T.
\tag{10}
$$

Similarly a statement of the conservation of linear momentum of the colliding system would be that

$$
m_D v_D + m_R v_R = m_T v_T.
\tag{11}
$$

The question is: are these statements *true* for the wave experiment and our definitions? That the first is true is verifiable by substituting equations (9) into equation (10), obtaining the expected wave relationship

$$
1 + R = T.
\tag{12}
$$

That the second is true we may likewise immediately verify by comparison:

$$
m_D v_D + m_R v_R = \frac{1}{c_0} \left(\frac{c_1 + c_0}{c_1 + c_0} - \frac{c_1 - c_0}{c_1 + c_0} \right) = \frac{2}{c_1 + c_0},
\tag{13}
$$

and

$$
m_T v_T = \frac{1}{c_1} \left(\frac{2 c_1}{c_1 + c_0} \right) = \frac{2}{c_1 + c_0}.
\tag{14}
$$

Amplitude & mass and acoustic boundary conditions

We may obtain some sense of why the amplitude/mass and slowness/velocity associations produce this particle and wave relationship by reviewing what happens to waves at boundaries. Consider a wave of unit amplitude moving at speed c_0 in the positive z direction. It is incident from above ($z < 0$) upon an interface, at $z = 0$, below which waves

---

*One potentially unedifying consequence of this interpretation of the amplitude is that we must accept the possibility of an object with negative mass, since for instance $R < 0$ when $c_1 < c_0$. But, however one might feel about this, if we allow $m < 0$ when appropriate, then the above rules correctly represent reflection and transmission through all possible combinations of c_0 and c_1.

propagate with speed c_1. In addition to this incident wave, there will be a transmitted wave and a reflected wave:

$$P(z < 0, \omega) = A \exp\left(i\frac{\omega}{c_0}z\right) + B \exp\left(-i\frac{\omega}{c_0}z\right), \tag{15}$$

$$P(z > z_1, \omega) = C \exp\left(i\frac{\omega}{c_1}z\right), \tag{16}$$

whose derivatives in the z direction are

$$P'(z < 0, \omega) = A\left(i\frac{\omega}{c_0}\right) \exp\left(i\frac{\omega}{c_0}z\right) + B\left(-i\frac{\omega}{c_0}\right) \exp\left(-i\frac{\omega}{c_0}z\right), \tag{17}$$

$$P'(z > z_1, \omega) = C\left(i\frac{\omega}{c_1}\right) \exp\left(i\frac{\omega}{c_1}z\right). \tag{18}$$

Acoustic, constant density boundary conditions require that the wave and its normal derivative, P and P' respectively, be continuous across $z = 0$, i.e.,

$$1 + R = T \tag{19}$$

and

$$\left(\frac{1}{c_0}\right) + R\left(-\frac{1}{c_0}\right) = T\left(\frac{1}{c_1}\right), \tag{20}$$

if $R = B/A$ and $T = C/A$. Comparing equations (12)–(14) with (19) and (20), we see that the associations made in the previous section, of the *amplitude of the wave* with the *mass of a particle*, and the *slowness of the wave* with the *velocity of the particle*, reliably maps statements about wave conditions at a boundary into statements about mass and momentum conservation at a collision.

MULTIPLE INTERFACES: COLLISIONS AND DISINTEGRATIONS

Generalizing the results of the previous section to multiple interfaces is possible if time-reversed collisions, or *disintegrations*, are included as permissible phenomena. Figure 3 is a diagram depicting some of the wave paths which contribute to the field (again in a zero-offset VSP experiment) in the presence of two interfaces. Let us start analyzing the experiment by again transforming into the "z_g as time, t as space" framework.

The VSP experiment, from the point of view of the sensors, is a time-evolution of amplitudes over a fixed range of z_g values. This real-time process of data creation can be reproduced by sweeping a vertical line from left to right across Figure 3. The arrivals in the section would appear wherever the moving vertical line intersected any blue path in the diagram (assuming they have been sketched with slopes proportional to the medium velocities c_0, c_1 and c_2). A particle/collision view would have us instead draw a horizontal line at the top, and have it sweep downward.
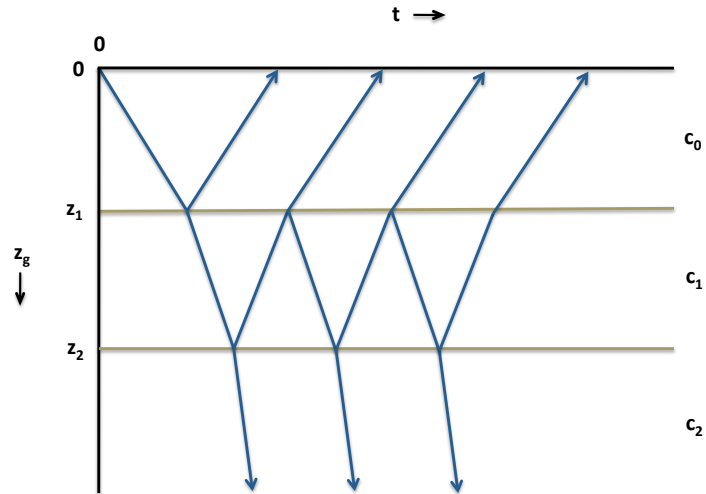
FIG. 3. A space vs. time diagram depicting some of the events in a zero-offset VSP experiment with two interfaces. The VSP data, as they would actually be measured in real time, are reproduced by a vertical line sweeping at a uniform rate from left to right. The collision model would instead involve a horizontal line sweeping downward.

Collisions at points of upward reflection

Consider first the three left-most legs in the diagram in Figure 3. These are highlighted in Figure 4. This portion of the experiment is locally identical to the single interface situation illustrated in Figure 1. The downward-sweeping horizontal line creates a trace at every "instant" z_g. If an arrival is placed wherever the blue lines and the horizontal line intersect, as the latter sweeps from low z_g to high, the apparent phenomenon of colliding "particles" depicted in Figure 2 is reproduced. Locally, the same momentum-conserving collision recurs.
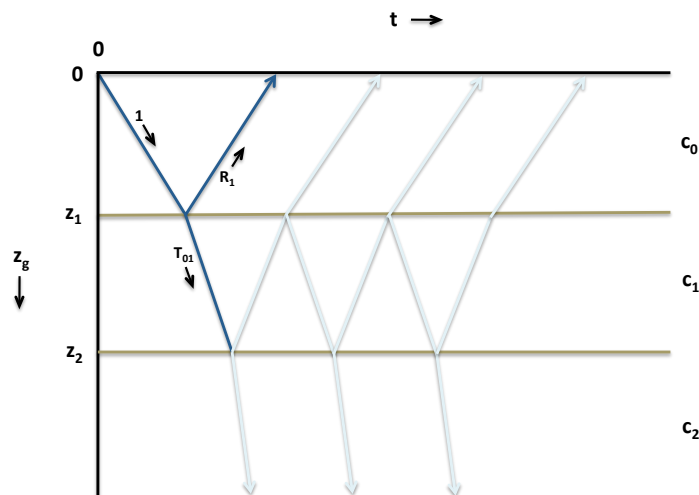

FIG. 4. The portion of the diagram depicting the momentum-conserving collision at the shallowest interface.

Disintegrations at points of downward reflection

The mass- and momentum-conservation holds for each of the many reflection/transmission interactions that occur. Consider, for instance, the upgoing wave incident on z_1 and its consequent reflection and transmission, highlighted in Figure 5. Using the reciprocal relationship again for the apparent velocities of the particles:

$$v_{\mathrm{D}} = -\frac{1}{c_1},$$
$$v_{\mathrm{R}} = \frac{1}{c_1}, \qquad (21)$$
$$v_{\mathrm{T}} = -\frac{1}{c_0},$$

and again associating the masses of the particles with the amplitudes of the three wave components:

$$m_{\mathrm{D}} = T_{01} R_2,$$
$$m_{\mathrm{R}} = -T_{01} R_2 R_1, \qquad (22)$$
$$m_{\mathrm{T}} = T_{01} R_2 T_{10},$$

where R_n is the reflection coefficient at the nth interface and T_{mn} is the transmission coefficient associated with a wave crossing from medium m to medium n. We establish the mass conservation, assuming again that the amplitude of the waves are the masses of the particles, by noting that

$$m_{\mathrm{D}} + m_{\mathrm{R}} = T_{01} R_2 (1 - R_1) = T_{01} R_2 T_{01} = m_{\mathrm{T}}. \qquad (23)$$

The momentum conservation is similarly established by comparing

$$m_{\mathrm{T}} v_{\mathrm{T}} = T_{01} R_2 T_{10} \left(-\frac{1}{c_0} \right) = -T_{01} R_2 \frac{2}{c_0 + c_1}, \qquad (24)$$

which holds "before" (i.e., at z_g values less than the interface depth), and

$$
\begin{aligned}
m_{\mathrm{D}} v_{\mathrm{D}} + m_{\mathrm{R}} v_{\mathrm{R}} &= T_{01} R_2 \left[\left(-\frac{1}{c_1} \right) 1 + \left(\frac{1}{c_1} \right) (-R_1) \right] \\
&= -T_{01} R_2 \left(\frac{1}{c_1} \right) \left[\frac{c_1 + c_0}{c_1 + c_0} + \frac{c_1 - c_0}{c_1 + c_0} \right] \\
&= -T_{01} R_2 \frac{2}{c_0 + c_1},
\end{aligned}
\qquad (25)
$$

which holds "after" the collision.

In spite of this similarity, there is a significant difference between the interactions depicted in Figures 4 and 5. Within the particle/collision view, we experience the VSP experiment as if we were riding on a horizontal line moving from an early apparent time

z_g to a late apparent time z_g, hence the reflection-transmission process in Figure 5 happens in reverse order compared to that of Figure 4. That is, a single particle, drifting to the left, spontaneously disintegrates at apparent time $z_g = z_1$, after which two independent particles diverge from the point of the explosion, one going left and one going right, with linear momentum conserved. In general, to include both upgoing and downgoing waves interacting at interfaces, we must widen our allowed types of particle interaction to include momentum-conserving collisions *and* momentum-conserving disintegrations, i.e., collisions happening backwards in time.
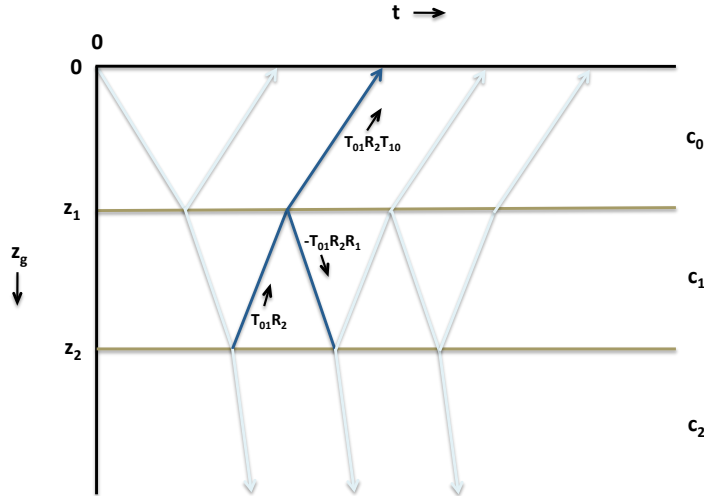

FIG. 5. The conservation of momentum as we have framed it holds for all incidence-reflection-transmission triplets.

We may view these processes taking place together by again making a movie in which we watch an interval of the time dimension evolve as we step from low values of z_g to high. The two-interface model depicted in Figure 1 has an infinite number of reflections, but, if we decide that wave components that have reflected two or more times are negligible, we can limit ourselves to following a tractable number of particles. Ten frames of the movie are shown in Figure 6. Two upgoing wave components, R_1 and R_2, corresponding to primary reflections, and one downgoing component, D, corresponding to the direct wave, are seen at low apparent time (z_g) values. These drift freely (i.e., without acceleration) towards each other as z_g approaches 400m, the depth of the first interface. At the interface, D and R_1 collide and stick together, and continue on as a unit thereafter. This is the interaction depicted in Figure 4. At the same apparent time, R_2 spontaneously disintegrates into two components, which drift away from each other. This is the interaction depicted in Figure 5. Both processes, as we have seen, conserve "mass" and "momentum".

Looking further ahead, it is interesting to note that the particle created by the collision of D and R_1 is destined to collide with one of the disintegrated parts of R_2, when z_g coincides with the second interface at 600m. We will return to this mingling of particles when we use the particle model to classify events.
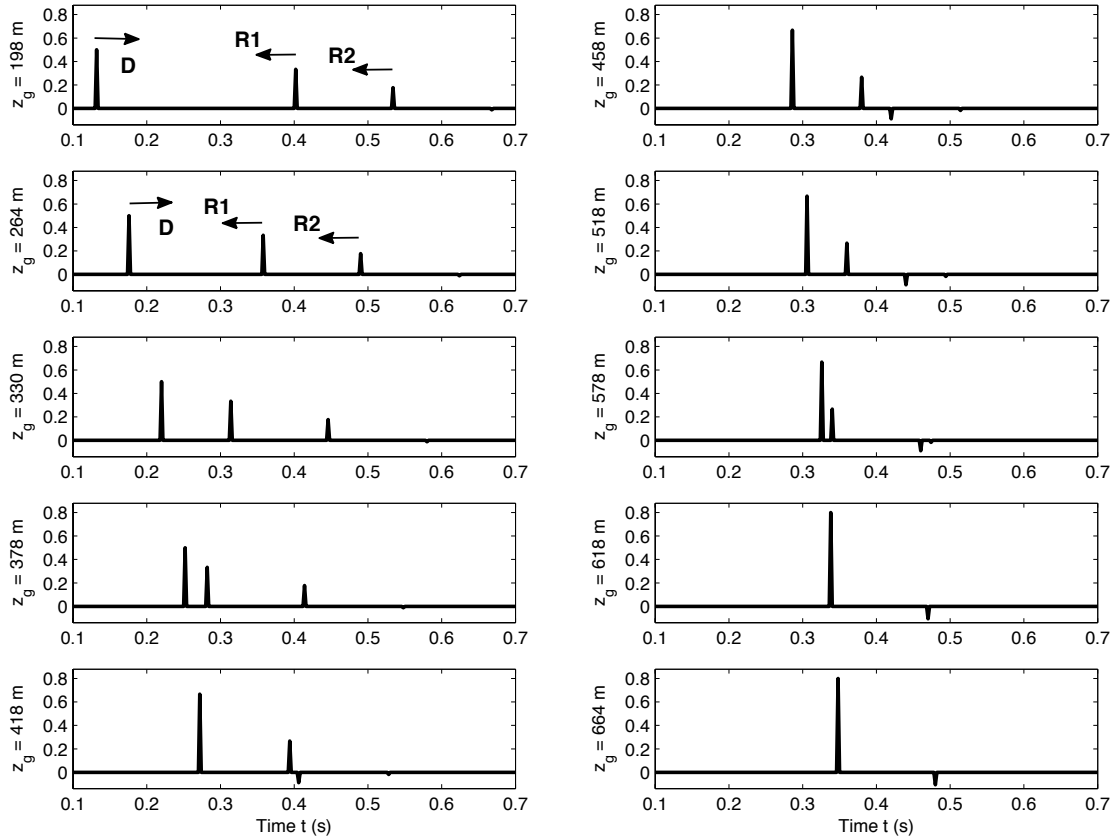
FIG. 6. Ten "movie frames" depicting the mechanical interaction of the 3+ particles associated with a two-interface VSP experiment. We sweep through "time" values (z_g) top-to-bottom on the left column, then top-to-bottom on the right column. In the first 4 frames, D and R_1 approach one another as z_g approaches the depth of the first interface, ultimately colliding and sticking together. In the following four frames, R_2 spontaneously disintegrates into two components, one of which drifts towards the agglomerate of D and R_1, and the two ultimately collide and stick together also. In the last two frames, the result of the two collisions and the result of the single disintegration drift at the same apparent velocity to the right. *NB: for display purposes, the direct wave, i.e., the leftmost event in each panel, has been reduced in amplitude by a factor of 0.5.*

HETEROGENEOUS MEDIA: PARTICLES MOVING IN A POTENTIAL FIELD

We next consider the case in which the media between reflectors (within which the wave components have, thus far, appeared to be particles free to drift at uniform apparent velocities) now contain smooth variations in the actual wave velocity $c(z_g)$. We shall see that the presence of a smooth velocity profile makes the particles in the VSP experiment act as if they were moving not freely but within a potential field. We shall establish a map between the actual wave velocity field $c(z_g)$ and the apparent field.

In Figure 7 the situation is illustrated: $c(z_g)$ is the actual velocity profile the wave experiences, expressed as a function of z_g, the actual depth variable expressing the location of the geophones in the well. Let us assume a wave of amplitude P_0 is propagating downward, i.e., in the positive z direction, through the profile.
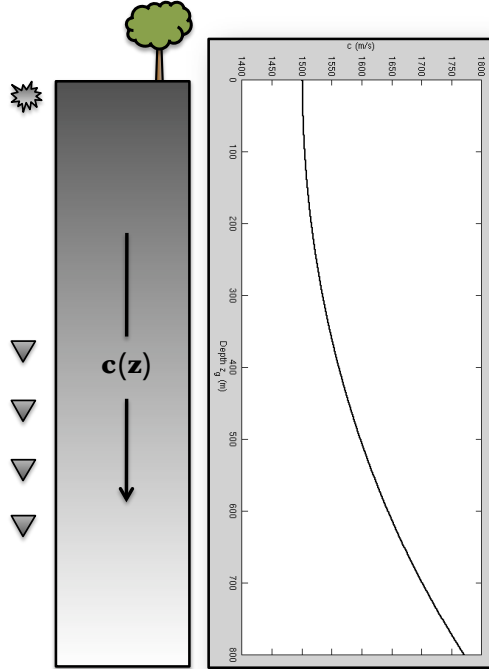
FIG. 7. Configuration of a VSP experiment in a medium with a smoothly-varying velocity profile $c(z_g)$.

Provided $c(z_g)$ is smooth, we may use the reciprocal relationship developed in earlier sections to produce an expression for the apparent velocity v with which the downgoing wave appears to drift as z_g increases:

$$v(z_g) = \frac{1}{c(z_g)}. \tag{26}$$

Let us, in fact, temporarily replace z_g with a different variable, τ, to remind us that we see it as an apparent time variable. If v is the velocity with which the component moves along an apparent space dimension (i.e., t), let us denote it further as $\dot{x}$, where x is a position along the time axis. With only a change in interpretation then, we have mapped the smooth background velocity model $c(z_g)$ to an apparent velocity $\dot{x}(\tau)$. From here it is relatively straightforward to determine the apparent force experienced by the particle, and thereafter its apparent potential energy. We integrate $\dot{x}(\tau)$ to determine the location of the particle x at a given τ (in real terms, its location along the time axis at a given depth in the well z_g), and we take its derivative to measure its acceleration:

$$
\begin{aligned}
x(\tau) &= \int_0^\tau \dot{x}(\tau')d\tau + x_0 \\
\ddot{x}(\tau) &= \frac{d}{d\tau}\dot{x}(\tau).
\end{aligned}
\tag{27}
$$

To determine the apparent forces acting to cause this motion, we need to know what the acceleration $\ddot{x}$ of the particle will be at a given position x. Inverting $x(\tau)$ in equation (27), we produce $\tau(x)$, which we substitute into $\ddot{x}(\tau)$ in the same set of equations, producing $\ddot{x}(x)$.

An unbalanced force acting on a particle can be expressed as the product of its mass and the acceleration the force causes. Since amplitude has usefully played the role of the mass thus far we suggest writing

$$F(x) = P_0 \ddot{x}(x), \tag{28}$$

where F is the apparent force field at location x along the trace. It is also then possible to say that the particle has the potential energy $V(x)$ where

$$V(x) = P_0 \int_0^x \ddot{x}(x') dx', \tag{29}$$

assuming no contributions are made to the potential from $x < 0$, and that there are no transport losses in amplitude.

Example

Let us work an example. Suppose we have a wave velocity profile of the form

$$c(z_g) = A' \sec B z_g, \quad 0 \le z_g \le z_M, \tag{30}$$

such that the apparent velocity of a direct wave with amplitude P_0 is

$$\begin{aligned} v(z_g) &= [c(z_g)]^{-1} \\ &= A \cos B z_g, \end{aligned} \tag{31}$$

where $A = A'^{-1}$. Suppose further that A, B, and z_M are chosen such that the amplitude of $c(z_g)$ begins at a reasonable number, say 1500m/s, and the singularity in the secant function is not encountered in the interval of interest. See the top left panel of Figure 8. Following the prescription above, we express the apparent velocity as

$$v(\tau) = A \cos B \tau, \tag{32}$$

as depicted in the middle row, left column of Figure 8, in which case, integrating,

$$x(\tau) = \frac{A}{B} \sin B \tau + x_0, \tag{33}$$

as depicted in the bottom row, left column of Figure 8, and, differentiating,

$$\ddot{x}(\tau) = -AB \sin B \tau, \tag{34}$$

as depicted in the top row, right column of Figure 8. We next invert equation (33), which provides us with $\tau(x)$:

$$\tau(x) = \frac{1}{B} \sin^{-1} \left[\frac{B}{A}(x - x_0) \right], \tag{35}$$

and substitute this into equation (34), to obtain

$$\ddot{x}(x) = -B^2(x - x_0), \tag{36}$$

as depicted in the middle row, right column of Figure 8 (since x is, in real terms, a position along the time axis, we have plotted it as a function of the real time t). If the wave passes $x = 0$ at $\tau = 0$ (i.e., if we choose to set $t = 0$ at the point when the wave passes $z_g = 0$), then $x_0 = 0$. With the acceleration of the particle as a function of position in hand, we use equation (28) to obtain the apparent force field

$$F(x) = -P_0 B^2 x \tag{37}$$

and potential

$$V(x) = \frac{P_0 B^2}{2} x^2, \tag{38}$$

in rough analogy to the problem of the motion of a harmonic oscillator. The potential is illustrated as a function of time (i.e., x interpreted in real terms as location along the trace, or time axis) in the bottom row, right column of Figure 8.

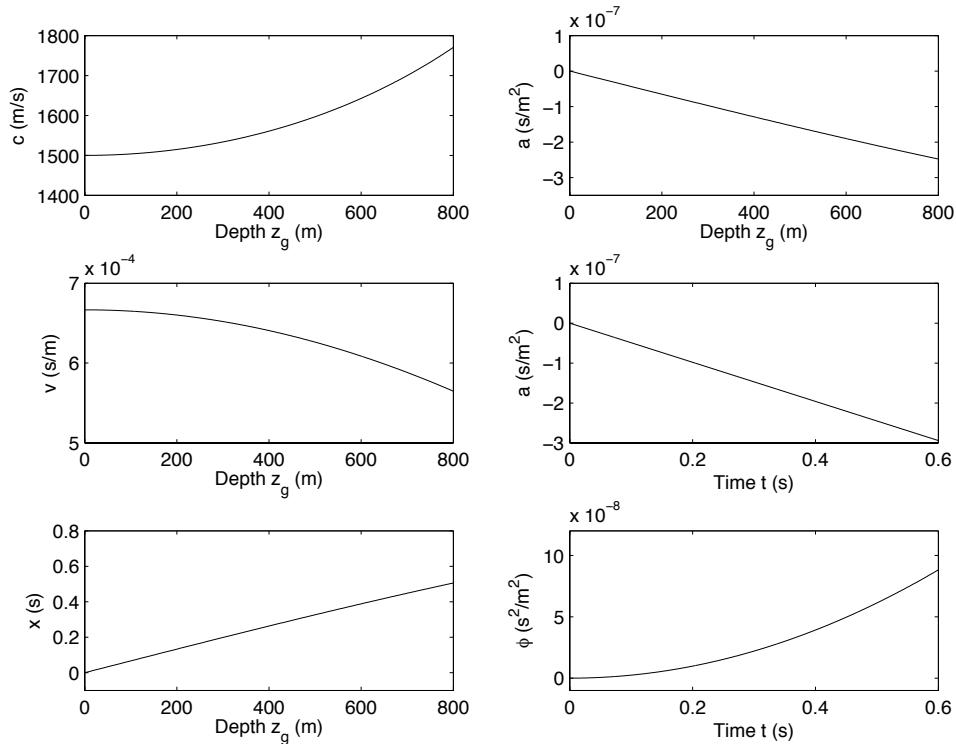
FIG. 8. Waypoints in the establishing of a map between wave velocity profile and apparent potential through which the VSP "particles" accelerate.

NON-ZERO OFFSET: ANOTHER POTENTIAL

In Figure 9 the geometry of a VSP experiment with nonzero offset is illustrated, including rays intersecting geophones both above and below the interface at z_I. Let us determine

what differences there are between this and the zero offset case in our conclusions about the particle model for a single interface VSP experiment. Much is the same: the data taken by a receiver at $z_g < z_1$ may be approximately modeled as

$$D(z_g < z_I, t) = 1 \times \delta(t - \tau_D) + R(\theta_i) \times \delta(t - \tau_R), \tag{39}$$

and the data taken by a receiver at $z_g > z_1$ as

$$D(z_g > z_I, t) = T(\theta_i) \times \delta(t - \tau_T). \tag{40}$$

The differences are that (1) the reflection and transmission coefficients are functions of angle, and (2) the relationship between the travel times and z_g, i.e., the functional forms of τ_D, τ_R and τ_T, are slightly more complicated. Indeed if we allow z_g to increase at a uniform rate we can hardly now expect to see the direct, reflected, and transmitted components of the wave drift with uniform apparent velocity along the time axis any longer.
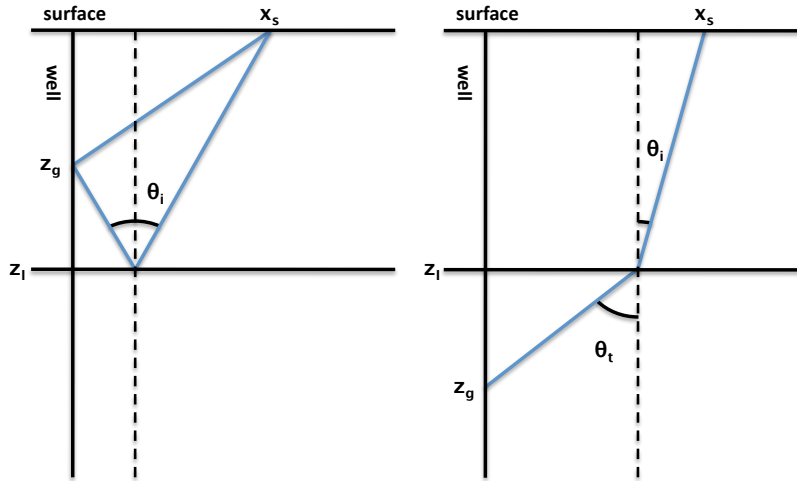

FIG. 9. Schematic of VSP experiment with offset.

Let us consider the travel times of the events first. In Appendices A & B, we derive formulas for θ_i and θ_t directly in terms of z_g and what we will consider fixed parameters of the experiment, x_s, z_I, and the P-wave velocities for the upper and lower media, c_0, and c_1 respectively. For the $z_g < z_I$ case, we have the tangent of the single angle of incidence/reflection θ_i

$$\sin \theta_i \approx \tan \theta_i = \frac{x_s}{2z_I - z_g}, \tag{41}$$

and for the $z_g > z_1$ case, we have the following approximation of the sine of the incidence angle, which can be easily converted to the sine of the transmission angle using Snell's law:

$$\sin \theta_i \approx \frac{c_0}{c_1 x_s}(z_I - z_g) - \frac{c_1}{c_0 x_s} z_g + \frac{c_0^2}{c_1^2 x_s} \left\{ \left[(z_g - z_I)\frac{c_1}{c_0} + z_I \right] + 2\frac{c_1^2}{c_0^2} x_s^2 \right\}^{1/2}, \tag{42}$$

and

$$\sin \theta_t = \frac{c_1}{c_0} \sin \theta_i. \tag{43}$$

From the diagram in Figure 9 we have that

$$
\begin{aligned}
\tau_D &= \frac{z_g}{c_0 \cos \theta_i} \approx \frac{z_g}{c_0} \left(1 + \frac{1}{2} \sin^2 \theta_i \right) \\
\tau_R &= \frac{2z_I - z_g}{c_0 \cos \theta_i} \approx \frac{2z_I - z_g}{c_0} \left(1 + \frac{1}{2} \sin^2 \theta_i \right) \\
\tau_T &= \frac{z_g}{c_1 \cos \theta_i} + \frac{z_g - z_I}{c_1} \approx \frac{z_g}{c_1} \left(1 + \frac{1}{2} \sin^2 \theta_i \right) + \frac{z_g - z_I}{c_1} \left(1 + \frac{1}{2} \sin^2 \theta_t \right).
\end{aligned} \tag{44}
$$

Eliminating the angles from equations (44) using equations (41)–(43), and taking the approximations ($\approx$) as read, we have

$$
\begin{aligned}
\tau_D(x_s, z_g) &= \frac{z_g}{c_0} \left[1 + F_1(x_s, z_g) \right] \\
\tau_R(x_s, z_g) &= \frac{2z_I - z_g}{c_0} \left[1 + F_1(x_s, z_g) \right] \\
\tau_T(x_s, z_g) &= \frac{z_g}{c_1} \left[1 + F_2(x_s, z_g) \right] + \frac{z_g - z_I}{c_1} \left[1 + F_3(x_s, z_g) \right],
\end{aligned} \tag{45}
$$

where

$$
\begin{aligned}
F_1 &= \frac{1}{2} \frac{x_s^2}{(2z_I - z_g)^2} \\
F_2 &= \frac{1}{2} \left[\frac{c_0}{c_1 x_s}(z_I - z_g) - \frac{c_1}{c_0 x_s} z_g - \frac{c_0^2}{c_1^2 x_s} \left\{ \left[(z_g - z_I)\frac{c_1}{c_0} + z_I \right] + 2\frac{c_1^2}{c_0^2} x_s^2 \right\}^{1/2} \right]^2 \\
F_3 &= \frac{1}{2} \left[\frac{1}{x_s}(z_I - z_g) - \frac{c_1^2}{c_0^2 x_s} z_g - \frac{c_0}{c_1 x_s} \left\{ \left[(z_g - z_I)\frac{c_1}{c_0} + z_I \right] + 2\frac{c_1^2}{c_0^2} x_s^2 \right\}^{1/2} \right]^2.
\end{aligned} \tag{46}
$$

We may use these delay times to once again derive apparent velocities and potential energies of the particles.

<center>**SEISMIC EVENTS**</center>

As the subsurface within which a seismic wave propagates becomes more complicated, it becomes the secondary task of a data model to permit identification and characterization of portions of the field which contribute significantly vs. those which contribute negligibly to the measured data. In seismic exploration, of course, we speak of "events", direct waves, primaries, multiple reflections—coherent arrivals of wave energy to which we ascribe a history of propagations, reflections, and other interactions. Let us discuss the expression of an event in our simple VSP data set from the point of view of colliding particles.

To do so it is sufficient to consider a two-interface medium, such as that depicted in Figure 3. In that figure some of the paths taken by a seismic wave as it propagates, from $z_g = 0$ to some point along the z_g axis, are illustrated. To extract from this diagram one event, for instance *the portion of the field that reflects upwards once at the boundary z_2*, is to focus our attention on a single path in this tree of paths, beginning at $(0, 0)$ and ending with an arrowhead, and excluding all others. This is illustrated in Figure 10.
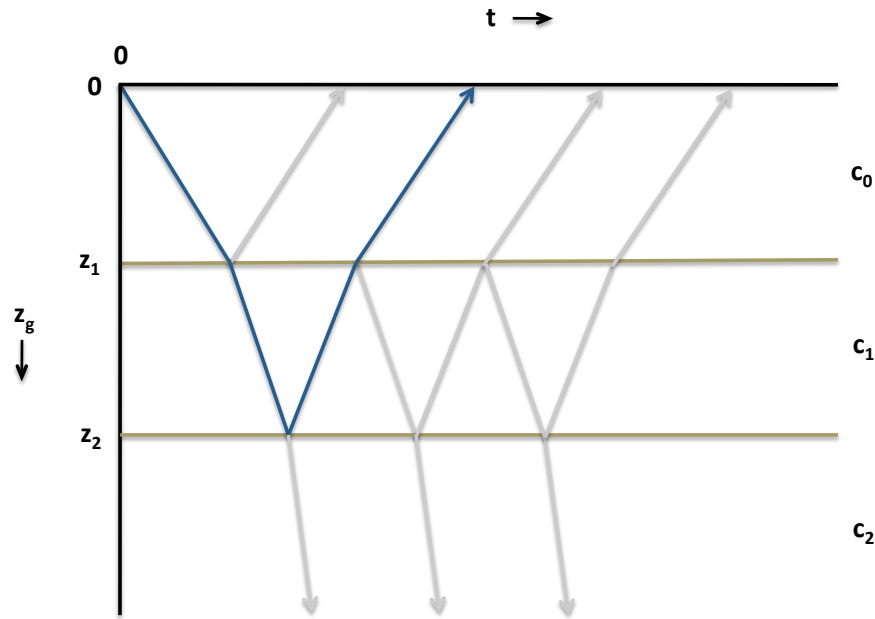

FIG. 10. Picking out an event from the full wave field amounts to focusing on one of the many paths illustrated here, beginning at $(0, 0)$ and ending at an arrowhead. The primary reflecting from the interface at z_2 is highlighted in blue. Notice that within the particle/collision view, in which z_g plays the role of time, half of the path, or "world line" of the primary, propagates backwards in time, that is, moves in a $-z_g$ direction.

Events as single particles moving forwards and backwards in time

Our definition of an event involves, in other words, what in other fields might be called the "world-line" of the wave component: a path (the blue line in the figure) which accounts for the full history of the event, over all times and locations. A striking aspect of how the world line of an event appears, from the point of view of the particle/collision model, in which z_g is considered a time variable, is visible in the example in Figure 10. Half of it—the upgoing leg—is apparently moving backwards in time. Evidently if we allow ourselves to perceive the entire history of the event, then from the point of view of the particle model the event is a single object that moves sometimes forwards and sometimes backwards in time.

Events as multiple interacting objects moving forwards in time

But one of the other stipulations of the particle/collision model denies us a world-line view of the VSP experiment, in which we observe "from the outside" the entire time and

space history of the experiment, as we do when we contemplate a picture like that in Figure 10. The model constrains us to experience z_g as if it were a time variable elapsing at a uniform rate, so everything has to go forwards. How does an event whose world-line moves both forwards and backwards in apparent time appear to someone who is constrained to see everything unfold in one temporal direction? It takes on the appearance of a multiplicity of interacting particles that are spontaneously produced and annihilated in collisions. Let us expand on this by considering the case of a transmitted multiple; the basic behaviour of all other events follows.

Multiples: spontaneous pair productions and annihilations

The entire time and space history of an event classified as a first order internal multiple is depicted in Figure 11. It is first-order in the sense that it has experienced a single upward reflection during the course of its propagation history. The question we will consider is: what do we see occurring in the collision movie, if all wave components not associated with this multiple event are suppressed?
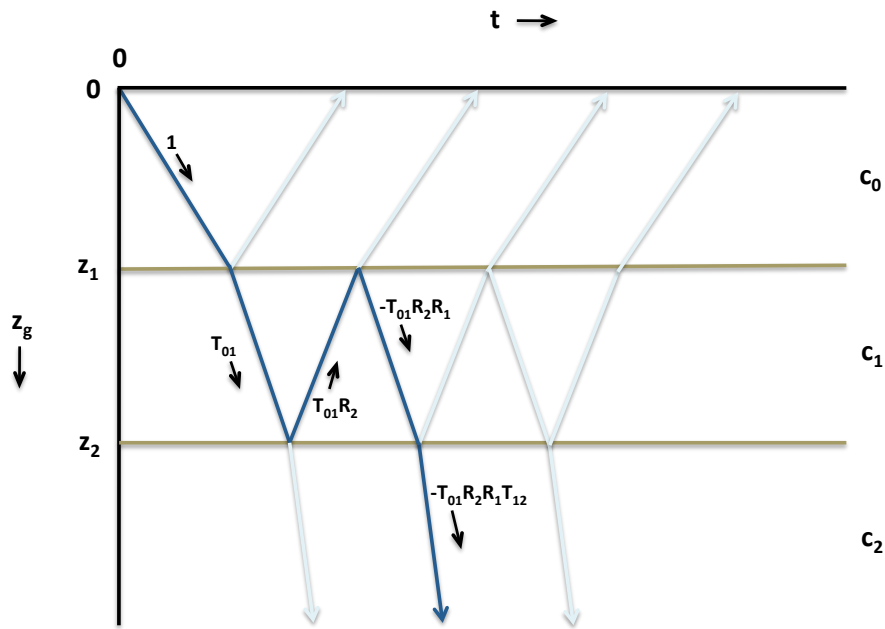
FIG. 11. An *event* as it is expressed within the collision model is an arrival with a definite propagation history. It appears as a line diagram of the wave path over the course of its various reflection and transmission interactions. Depicted here is a first order transmitted multiple. The event seen over the totality of t and z_g, in which z_g is treated as a time variable, appears as a single entity which travels sometimes forwards and sometimes backwards in time.

Eliminating all other events, the multiple in the three regions occupied by z_g during its

progress from low to high values is expressible mathematically as:

$$D_{\mathrm{M}}(z_g, t) = \begin{cases} 1 \times \delta\left(t - \frac{z_g}{c_0}\right), & z_g < z_1 \\[2mm] T_{01}\delta\left(t - \frac{z_1}{c_0} - \frac{z_g - z_1}{c_1}\right) & \\[1mm] +T_{01}R_2\delta\left(t - \frac{z_1}{c_0} - \frac{2z_2 - z_1 - z_g}{c_1}\right) & \\[1mm] -T_{01}R_1R_2\delta\left(t - \frac{z_1}{c_0} - 2\frac{z_2 - z_1}{c_1} - \frac{z_g - z_1}{c_1}\right), & z_1 < z_g < z_2 \\[2mm] T_{01}T_{10}\delta\left(t - \frac{z_1}{c_0} - \frac{z_2 - z_1}{c_1} - \frac{z_g - z_2}{c_2}\right), & z_2 < z_g \end{cases} \tag{47}$$

The arguments of the delta functions in equation (47) describe apparent particle motion. As z_g progresses from 0 towards z_1, a single particle drifts to the right with velocity $1/c_0$. At $z_g = z_1$, the one particle suddenly becomes three. How does this occur? We may resort to either the math in equation (47) or the movie, depicted in Figure 12, which is created by a horizontal line sweeping downward over Figure 11). The single particle prior to apparent time $z_g = z_1$ appears to spontaneously decelerate as it crosses z_1, but it is essentially contiguous with the particle in the first line of the $z_1 < z_g < z_2$ case in equation (48): this is apparent since the arguments of that delta function and the one in the $z_g < z_1$ case coincide as $z_g \to z_1$. Schematically, the two are expressed through the crooked line $1 \to T_{01}$ at the left of Figure 11.

The other two events in the $z_1 < z_g < z_2$ case appear spontaneously, collocated at time $t = z_1/c_0 + 2(z_2 - z_1)/c_1$, and diverge thereafter, one with velocity $1/c_1$ and the other with velocity $-1/c_1$. Now within the layer, the three particles drift with the same speed $|1/c_1|$, two in the positive t direction and the other in the negative t direction. In fact, two of the particles are on a collision course, and annihilate at apparent time $z_g = z_2$. At the same instant (depth, in real terms), the rightmost particle spontaneously decelerates once again, and finally drifts on, still to the right, as z_g grows beyond z_2. An imagined horizontal line sweeping downward in diagram in Figure 11, intersecting with the dark blue event diagram, depicts the pair creation and annihilation quite clearly.

All first order transmitted multiples have this characteristic expression in the particle/collision model: one particle drifts alone, to be eventually joined by two more which spontaneously appear, until one of the new particles annihilates with the original particle, leaving the remaining produced particle to drift alone. Similarly, a primary consists of two incident particles which annihilate at the "time" associated with the depth of the generating reflector, higher order multiples consist of larger numbers of sequential pair productions and annihilations, and so on. Events, in the particle/collision model, are distinguished based on number and interaction of contributing particles.

Since we have extinguished portions of the field not directly contributing to a given event, in general the particle interactions associated with events are neither momentum nor mass conserving.
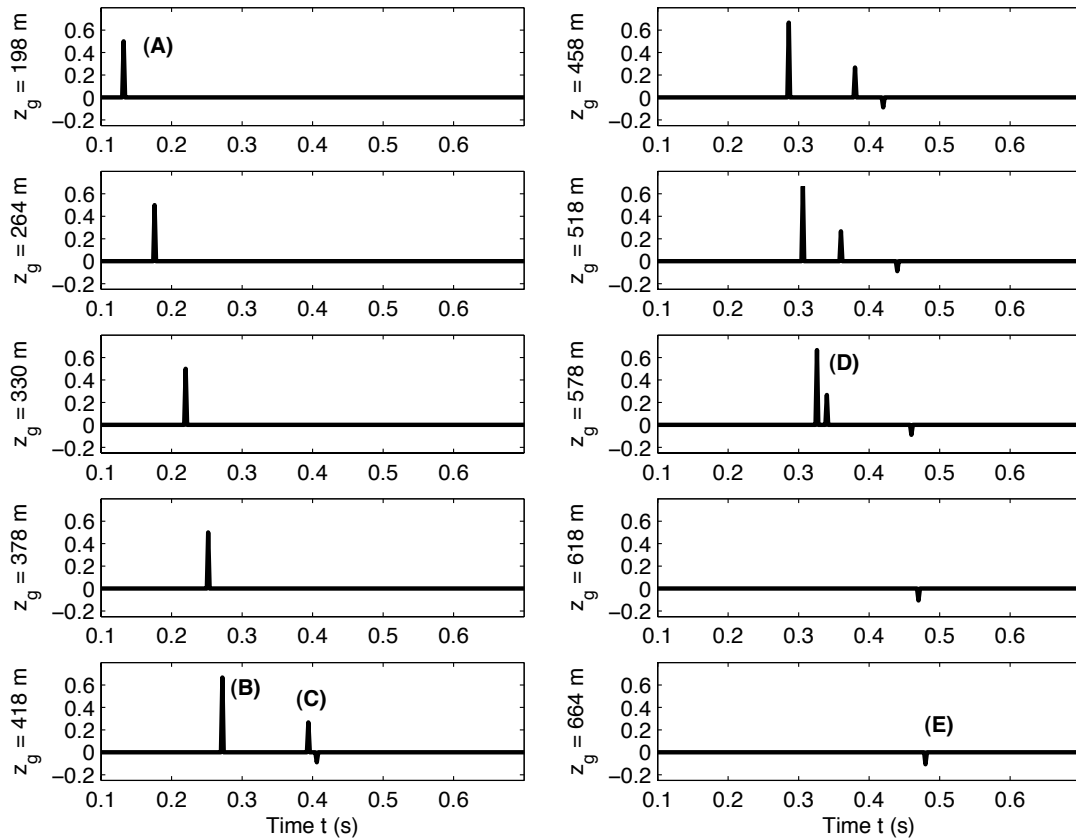
FIG. 12. Frames from the "movie" of the three particles whose interaction is characteristic of a first order transmitted multiple. In Figure 11 we saw the multiple as a single entity, a sequence of line segments depicting propagation forwards and occasionally backwards in "time". To view it entirely in terms of particles colliding, we constrain "time", i.e., z_g to move "forwards", hence we do not discern time-reversed processes as straightforwardly as this. Instead, we perceive it as three interacting particles, all moving forwards in time, but in different directions. In this Figure we see ten snapshots of the collision model "movie" of the process. At $z_g < z_1$, labelled (A), the multiple consists of a single particle drifting to the right. At time $z_g = z_1$, which here is 400m, it decelerates (B) and there is a sudden spontaneous production of two more particles (C), one drifting to the right and one to the left. The original, now decelerated particle and the left-going newly created particle approach one another, ultimately colliding and annihilating (D) at time $z_g = z_2$. The right-going particle continues to drift in that direction (E).

CONCLUSIONS

To conclude, let us speculate about practical, applied geophysics consequences of taking a particle/collision view of the seismic experiment. Perhaps there are none; but four points stand out. First, the particle/collision model is a space and time domain model. Second, primaries have a specific particle-interaction character within the model, that is they are distinguished from other events by the uniquely "primary-like" interactions they undergo. Third, there is a correspondence between the apparent times of the primary particle collisions/annihilations and the depths of interfaces. And fourth, the act of moving in the positive direction along the depth axis has the hallmarks of wavefield continuation. Given these points, it seems plausible and even likely that reverse-time imaging of primaries, and

the various associated imaging conditions could be usefully studied in particle/collision terms.

APPENDIX A: CALCULATION OF REFLECTION ANGLE

We are given the following problem. A source at the Earth's surface ($z = 0$) offset from the well by a distance x_s is ignited. The wave energy reflects at an interface at depth z_I, and is measured at a geophone at depth z_g in the well. The Earth is completely homogeneous above the interface. Assuming Snell's law holds, determine the angle of incidence/reflection θ explicitly in terms of x_s, z_g, and z_I. The ray, the interface, and the well are pictured in Figure 13 in blue, gray, and black respectively.
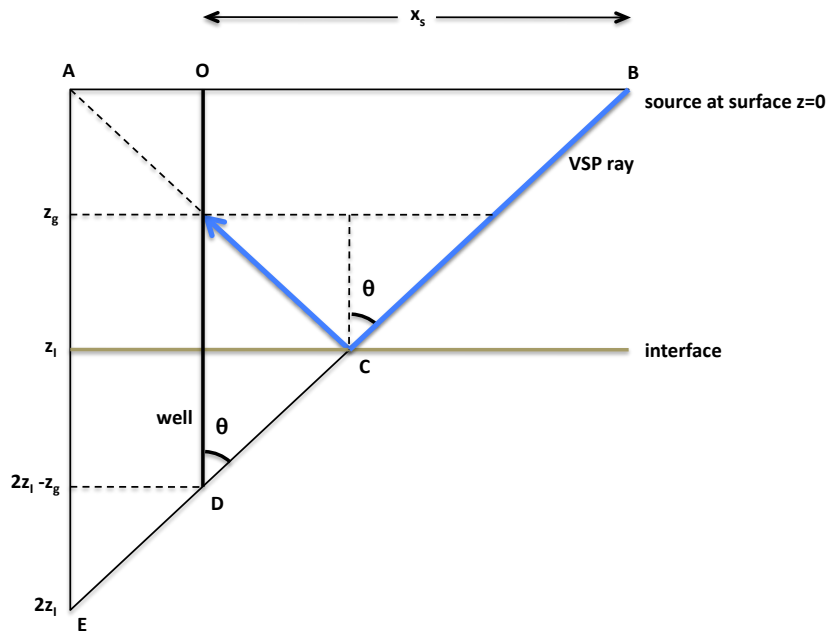
FIG. 13. Geometric determination of the incidence/reflection angle.

An algebraic solution is as follows. If L_S is the upward moving portion of the reflected ray and L_L is the downward moving portion of the ray, then we have

$$L_S \cos \theta = z_I - z_g \tag{48}$$

and

$$L_L \cos \theta = z_I, \tag{49}$$

or, adding the two,

$$L_S + L_L = \frac{1}{\cos \theta} (2z_I - z_g). \tag{50}$$

Furthermore

$$
\begin{aligned}
x_s &= 2L_L \sin \theta - (L_L - L_S) \sin \theta \\
&= L_L \sin \theta + L_S \sin \theta,
\end{aligned} \tag{51}
$$

hence

$$L_L + L_S = \frac{x_s}{\sin \theta}. \tag{52}$$

From equations (50) and (52), we therefore have that

$$x_s = (2z_I - z_g)\frac{\sin \theta}{\cos \theta}, \tag{53}$$

or

$$\theta = \tan^{-1}\left(\frac{x_s}{2z_I - z_g}\right). \tag{54}$$

A geometrical solution is as follows. We shall construct several triangles, consulting Figure 13. First, extend the upgoing ray such that it appears to return to the surface, forming triangle ACB. Then, create triangles AEB and AEC by extending the downgoing ray such that it coincides laterally with A. The length of the line AE is twice the depth of the interface at z_I. A third triangle ODB has also now been formed by the well and the extension of the downgoing ray. The angle θ at D is equal to the angle of incidence/reflection, since they are formed by the line DC included between two vertical lines. From the symmetry of the isosceles triangle AEC, the line OD, which cuts line AC at depth z_g, must also cut line EC at depth $2z_I - z_g$. Since the horizontal length OB is x_s, the angle θ at D, and therefore also the angle of incidence/reflection, and the expression for θ in equation (54) is recovered:

$$\theta = \tan^{-1}\left(\frac{x_s}{2z_I - z_g}\right). \tag{55}$$

APPENDIX B: CALCULATION OF TRANSMISSION ANGLE

A source at the Earth's surface ($z = 0$) offset from the well by a distance x_s is ignited. The wave energy transmits through an interface at depth z_I, and is measured at a geophone at depth $z_g > z_I$ in the well. The Earth is completely homogeneous above and below the interface, with P-wave velocities of c_0 and c_1 respectively. Assuming Snell's law holds, determine the angles of incidence θ_i and transmission θ_t explicitly in terms of x_s, z_g, and z_I and the velocities c_0 and c_1. The ray, the interface, and the well are pictured in Figure 14 in blue, gray-green, and black respectively.

A solution is as follows (consult Figure 14). We construct either of two triangles, the first, OBA, generated by extending the transmitted portion of the ray to the surface, and the second, ODC, by extending the incident portion of the ray to the well. We may proceed by analyzing either of these two triangles; we will use the first.

The following trigonometric relationships are apparent from the Figure. Since BC is a straight ray included between the parallel lines $z = 0$ and z_I, it makes the angle θ_t from the vertical at B, hence

$$\tan \theta_t = \frac{x_2}{z_g}. \tag{56}$$

FIG. 14. Geometric determination of the incidence/transmission angle.

If L_0 is the length of the incident portion of the ray (namely AO), we also have that

$$z_I = L_0 \cos \theta_i. \tag{57}$$

Finally, within the triangle AOB, the law of sines provides the relationship

$$\frac{\sin(\theta_t - \theta_i)}{x_2 - x_s} = \frac{\sin(\frac{\pi}{2} - \theta_t)}{L_0}, \tag{58}$$

or, simplifying and using the trigonometric addition formulas,

$$\frac{\cos \theta_t}{L_0} = \frac{\sin \theta_t \cos \theta_i - \cos \theta_t \sin \theta_i}{x_2 - x_s}. \tag{59}$$

Using equations (56) and (57) to eliminate L_0 and x_2 from equation (59), we have

$$(z_g \tan \theta_t - x_s) \cos \theta_t = (\sin \theta_t \cos \theta_i - \cos \theta_t \sin \theta_i) (\cos \theta_i)^{-1} z_I. \tag{60}$$

We next express this as an exact equation in a single unknown, $\sin \theta_i$, using in particular Snell's law $\sin \theta_t = (c_1/c_0) \sin \theta_i$:

$$(z_g - z_I) \frac{c_1}{c_0} \sin \theta_i + \left(1 - \frac{c_1^2}{c_0^2} \sin^2 \theta_i\right)^{1/2} \left[z_I \sin \theta_i (1 - \sin^2 \theta_i)^{-1/2} - x_s\right] = 0. \tag{61}$$

Since this has no simple solution we shall make a small angle approximation. We will begin with a *very* small angle approximation for the sake of analysis, namely that terms in $\sin^2 \theta_i$ or higher are negligible, in which case, expanding the powers of $1/2$ in binomial series and truncating, we have

$$\sin \theta_i = \frac{x_s}{(z_g - z_I)\frac{c_1}{c_0} + z_I}. \tag{62}$$

Referring again to Figure 14 we can see that the approximation in equation (62) is a deviation, based on Snell's law, away from a straight-ray model. In the limit $c_1 \to c_0$ the deviation vanishes, and equation (62) takes on the correct form $\sin \theta_i = x_s/z_g$. The ratio c_1/c_0 creates a new, effective triangle in which (if $c_1 > c_0$), the vertical edge is slightly longer than z_g, shrinking θ_i as is expected in refraction.

With that analysis complete, and noting that in the body of this paper we make approximations accurate to second order in $\sin \theta_i$ and $\sin \theta_t$, we proceed by increasing the accuracy of the approximation of $\sin_i \theta$ to match that of the other calculations. Carrying out the same expansion as above, and retaining terms up to $\sin^2 \theta_i$ results in the quadratic equation

$$\left[\frac{1}{2} \frac{c_1^2}{c_0^2} x_s \right] \sin^2 \theta_i + \left[(z_g - z_I) \frac{c_1}{c_0} + z_I \right] \sin \theta_i + [-x_s] = 0. \tag{63}$$

This has the general solution

$$\sin \theta_i = \frac{(z_I - z_g)\frac{c_1}{c_0} - z_I \pm \left\{ \left[(z_g - z_I)\frac{c_1}{c_0} + z_I \right]^2 + 2\frac{c_1^2}{c_0^2}x_s^2 \right\}^{1/2}}{\frac{c_1^2}{c_0^2}x_s}. \tag{64}$$

In both the limit $x_s \to 0$ and the limit $c_0 \to c_1$, equation (64) can be seen to reduce properly (i.e., to nil and x_s/z_g respectively) only if we choose the positive solution. Hence we have as our final formula

$$\sin \theta_i = \frac{(z_I - z_g)\frac{c_1}{c_0} - z_I + \left\{ \left[(z_g - z_I)\frac{c_1}{c_0} + z_I \right]^2 + 2\frac{c_1^2}{c_0^2}x_s^2 \right\}^{1/2}}{\frac{c_1^2}{c_0^2}x_s}, \tag{65}$$

which implies, for the transmission angle,

$$\sin \theta_t = \left(\frac{c_1}{c_0} \right) \frac{(z_I - z_g)\frac{c_1}{c_0} - z_I + \left\{ \left[(z_g - z_I)\frac{c_1}{c_0} + z_I \right]^2 + 2\frac{c_1^2}{c_0^2}x_s^2 \right\}^{1/2}}{\frac{c_1^2}{c_0^2}x_s}. \tag{66}$$